Fast Simulation of Large Networks of Nanotechnological and Biochemical Oscillators for Investigating Self-Organization Phenomena

Xiaolue Lai and Jaijeet Roychowdhury
Department of Electrical and Computer Engineering, University of Minnesota
Email: {laixl, jr}@ece.umn.edu

Abstract— **We address the problem of fast and accurate computational analysis of large networks of coupled oscillators arising in nanotechnological and biochemical systems. Such systems are computationally and analytically challenging because of their very large sizes and the complex nonlinear dynamics they exhibit. We develop and apply a nonlinear oscillator macromodel that generalizes the well-known Kuramoto model for interacting oscillators, and demonstrate that using our macromodel provides important qualitative and quantitive advantages, especially for predicting self-organization phenomena such as spontaneous pattern formation. Our approach extends and applies recently-developed computational methods for macromodelling electrical oscillators, and features both phase and amplitude components that are extracted automatically (using numerical algorithms) from more complex differential-equation oscillator models available in the literature. We apply our approach to networks of Tunneling Phase Logic (TPL) and Brusselator biochemical oscillators, predicting a variety of spontaneous pattern generation phenomena. Comparing our results with published measurements of spiral, circular and other pattern formation, we show that we can predict these phenomena correctly, and also demonstrate that prior models (like Kuramoto's) cannot do so. Our approach is more than 3 orders of magnitude faster than techniques that are comparable in accuracy.**

I. Introduction

Coupled self-oscillating systems appear in diverse natural and physical systems. For example, in nanoelectronics, the tunneling phase logic (TPL) [1], [2] device, which makes use of the bistability of single-electron tunneling oscillation to realize logic in phase are proposed for large scale circuits, due to its extremely high gate density and ultra low power dissipation. This concept has been applied [3] to implement cellular nonlinear networks (CNN) [4], [5], with ultra-high integration levels far beyond even DSM CMOS. Such CNN systems, consisting of large populations of interacting TPL oscillators, constitute a promising approach for implementing future large-scale high performance image processing systems.

It has long been known empirically that in systems of coupled oscillating entities, self-organizing collective behavior begins to occur when coupling exceeds a certain threshold; some entities start to synchronize spontaneously while others remain incoherent. Such "co-operation" and "competition" engendered by oscillatory nonlinear dynamics can produce complicated and beautiful spatio-temporal patterns of collective behavior. In particular, pattern formation arising from the nonlinear interaction of many individual cells in biochemical systems is a fascinating and extensively noted phenomenon (*e.g.*, [6]–[8]) — for example, an important issue in developmental biology is understanding the formation of spatial patterns in the embryo. These patterns can be explained by reaction diffusion theory [9], which shows that a system of reacting and diffusing chemicals can evolve spontaneously, from an initially uniform or random state, into spatial patterns known as Turing structures [9]. Such a process can be modeled as a network of biochemical oscillators interacting with each other. A typical example is the Brusselator reaction-diffusion system [10], whose patterns have recently been studied by experiments and simulation, especially under periodic perturbations [11], [12].

Although the dynamics of coupled oscillating systems have been well studied experimentally, analytical understanding of the details of pattern formation remains a challenge. A fundamental difficulty is that while it is often possible to understand specific systems of a few coupled oscillators at an analytical level, collective self-organization typically manifests itself only when *large numbers* of oscillators are networked. Many important characteristics of such large networks have been essentially impossible to understand fully using hand analysis so far, in part because pattern generation is often very sensitive to small details of the nature of and coupling between individual network entities [13], [14]. Thus, analytical simplifications that may be justified for small systems are potentially inapplicable to much larger ones and can lead to egregious mispredictions. As a result, accurate and detailed computational techniques are particularly critical for developing "understanding" of such systems. Because of the huge sizes and complex dynamics of these oscillatory networks, however, the computational problem is very challenging.

A straightforward computational method for nonlinear systems is to use numerical differential equation solvers to simulate waveforms in the time domain. But while such "transient" methods work well for non-oscillatory systems, they are far less suitable for simulating oscillators, especially coupled oscillators, due to inherent error buildup in phase. Very small timesteps have to be taken within each oscillation cycle and a complex integration methods need to be used to provide acceptable accuracy over long simulations. These problems are very familiar to circuit designers using simulation programs like SPICE [15] on oscillators, even though conventional electronic oscillator systems are usually very small relative to networks of nano and biochemical oscillators. Because envelopes and phase transition in oscillatory systems can evolve very slowly over thousands or millions of cycles, the computational challenge is dramatically exacerbated.

An extensive and deep literature is available on analytical approaches for understanding coupled oscillator systems; here, we provide a very brief synopsis of the main approaches in order to better place our contributions. One of the earliest studies was made by the legendary Norbert Wiener [16], [17], who studied collective synchronization phenomena using a Fourier-integral-based method. Later, Winfree formulated an equation governing phase transitions in populations of coupled limit-cycle oscillators and presented the concept of a phase sensitivity function [18]. Winfree's approach was abstracted by Kuramoto and applied to systems of identical oscillators with equally weighted, all-to-all, purely sinusoidal couplings, resulting in a well-known phase-based nonlinear differential equation model for coupled oscillator systems, the *Kuramoto model* [19], [20].

Using his model, Kuramoto developed a steady-state 'locking' (or 'drifting') condition which has been shown to successfully predict bifurcation of phase transitions in coupled oscillator systems. Kuramoto's model has been extremely influential because it has provided a relatively simple means of understanding self-organizing phenomena in systems of coupled oscillators. For predicting detailed pattern formation in a variety of real systems, however, Kuramoto's approach has accuracy limitations that can compound, in large networks, to the extent that wrong patterns can emerge, as we show in this paper.

The main contribution of this work is a much more powerful model that alleviates the lack of accuracy and general applicability of Kuramoto's model, while retaining its advantages of relative simplicity and computational efficiency; and indeed, significantly enhancing the convenience and ease with which the model can be specialized for any specific system of interest. Our model consists of nonlinear phase macromodel, together with amplitude macromodel that capture dominant amplitude components. The nonlinear phase macromodel is a scalar, nonlinear differential equation for phase deviations. A fundamental mechanism in collective synchronization is phase pulling/locking between oscillators; our phase macromodel captures these phenomena very effectively [21], [24].

In some situations (*e.g.*, strong loading effects due to coupling, unlocked mutually pulling oscillators, *etc.*), amplitude variations are large and couple significantly with phase effects, hence it is necessary to take them into account. To do so, we incorporate an amplitude macromodel [21] together with our phase equations. Thus, we are able to predict a much broader range of coupled oscillatory phenomena, with better accuracy than when using the phase macromodels alone. We develop models of common coupling mechanisms between

0-7803-9451-8/06/$20.00

oscillators that capture both phase and amplitude implications.

Importantly, both phase and amplitude macromodels can be extracted from the oscillators' differential equations automatically via numerical algorithms, making this method very easily applicable to a diverse variety of large and complex oscillator systems.

We apply and validate our technique on networks of biochemical and nanoelectronical oscillators: a large coupled Brusselator chemical dynamics system [10] and TPL-based cellular nonlinear network (CNN) [3]. We show that our methods are able to reproduce the formation of two important patterns families in biochemical systems: target patterns and spiral wave patterns, showing that they closely match measurements reported in the literature [6]–[8]. Furthermore, we show that Kuramoto's model is unable to predict the correct patterns. For the TPL network, we validate bistability behavior and demonstrate image processing ability (*e.g.*, edge detection) in the TPL-CNN system, predicting patterns very close to measurements reported in [3]. Our methods provide speedups of more than 3 orders of magnitude over direct time-stepping simulation of the original oscillator network.

The remainder of the paper is organized as follows: in Section II, we review the Winfree and Kuramoto models for the analysis of collective synchronization in coupled systems. In Section III, we summarize the nonlinear oscillator macromodel that we employ in this work. In Section IV, we describe our nonlinear macromodel-based technique for simulating coupled oscillating systems. Finally, in Section V, we present applications to the TPL-CNN and biochemical Brusselator systems.

II. Review of Previous Work

In this section, we summarize relevant previous work in the analysis of coupled oscillator systems.

A. Winfree's Equation For Coupled Systems

For the study of phase dynamics in coupled systems, a fruitful approach, pioneered by Winfree in 1967 [18], is based on the intuition that if an oscillator is perturbed by an external input at a given moment, its phase change should equal to the product of the perturbation strength and a "phase sensitivity" of the oscillator at that moment. Based on this intuition, Winfree formulated the governing equation for a coupled oscillating system with the assumptions of weak coupling and nearly identical oscillators. His phase model is expressed by

$$\dot{\theta}_i = \omega_i + (\sum_{j=1}^{n} X(\theta_j))Z(\theta_i), \qquad i = 1,...,n, \tag{1}$$

where n is the number of oscillators in the system, θ_i is the phase of oscillator i, θ_j is the phase of oscillator j and ω_i is the free running frequency of oscillator i. $X(\theta_j)$ denotes the influence on oscillator i exerted by oscillator j, and $Z(\theta_i)$ is the phase sensitivity function of oscillator i.

The chief difficulty with Winfree's model is that no clear or convenient means is provided for obtaining the phase sensitivity functions, which is not easily obtained. As we show later in this paper, our approach completely resolves this issue.

B. Kuramoto's Model For Coupled Systems

Kuramoto extended and simplified Winfree's approach [19] by showing (using asymptotic expansion theory [22] and averaging) that the long-term phase dynamics of weakly-coupled simple-harmonic-type oscillators can be predicted using

$$\dot{\theta}_i = \omega_i + \sum_{j=1}^{n} \Gamma_{ij}(\theta_j - \theta_i), \qquad i = 1,...,n, \tag{2}$$

where n is the system size and Γ_{ij} are "interaction functions".

Obtaining the interaction functions faces the same difficulties as Winfree's phase sensitivity function. Kuramoto made simplifications using the assumption that the coupled system was made up of identical oscillators with equally weighted, all-to-all, and purely sinusoidal coupling, resulting in

$$\Gamma_{ij}(\theta_j - \theta_i) = \frac{K}{n}\sin(\theta_j - \theta_i), \qquad i = 1,...,n. \tag{3}$$

K is a coupling strength. The phase equation is thus simplified to

$$\dot{\theta}_i = \omega_i + \frac{K}{n}\sum_{j=1}^{n} \sin(\theta_j - \theta_i), \qquad i = 1,...,n. \tag{4}$$

To visualize the phase dynamics, Kuramoto introduced the complex order parameter

$$re^{i\psi} = \frac{1}{n}\sum_{j=1}^{n} e^{i\theta_j}, \tag{5}$$

where $r(t)$ is the radius which measures the phase coherence, and $\psi(t)$ is the average phase. Equating the imaginary part of (5), the right hand side of (4) can be rewritten as

$$\frac{K}{n}\sum_{j=1}^{n} \sin(\theta_j - \theta_i) = Kr\sin(\psi - \theta_i). \tag{6}$$

Thus, (4) becomes

$$\dot{\theta}_i = \omega_i + Kr\sin(\psi - \theta_i) \tag{7}$$

Kuramoto showed that the locking condition of oscillator i in a coupled system is

$$|\Delta\omega_i| \leq Kr, \tag{8}$$

where $\Delta\omega_i$ is the difference between the free-running frequency of oscillator i and the mean frequency of the coupled system.

As noted in the introduction, the simplifications inherent in Kuramoto's model makes its predictions questionable when applied to large systems of self-organizing oscillators.

III. Nonlinear Oscillator Macromodel

In this paper, we present a generally applicable approach for predicting nonlinear dynamics in coupled oscillating systems. Our method is based upon a nonlinear oscillator macromodel originally developed for predicting noise, injection locking and other phenomena in electrical oscillators [23], [24]. In this section, we briefly review the nonlinear oscillator macromodel we employ for the simulation of coupled oscillating systems.

A. Oscillator Phase Macromodel - Intuition

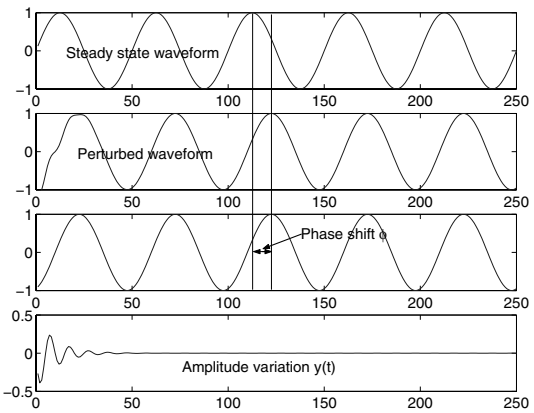

Fig. 1. Decomposition of phase and amplitude variation of oscillator under impulse perturbation.

Figure 1 depicts the decomposition of phase and amplitude variation of oscillators under impulse perturbation. The first figure is the steady state waveform of the oscillator without perturbation. The second figure depicts the waveform of the oscillator if an impulse perturbation is applied to the oscillator at $t = 0$: the oscillator features some transient amplitude variation which vanishes as time goes on, until finally, it converges to its steady state again, but with a permanent phase shift of ϕ. Intuitively, we know this perturbed waveform can be decomposed into a steady state waveform with the time shift ϕ, and the amplitude response $y(t)$, as shown in the third and fourth figure respectively. Since the amplitude response of a perturbed oscillator is stable, this implies that the impulse

response $y(t)$ should die out as time goes to infinity. As a result, the decomposition of the phase deviation ϕ and the amplitude response $y(t)$ should be unique, and the response of the perturbed oscillator can be represented as

$$x_p(t) = x_s(t+\phi) + y(t), \tag{9}$$

where $x_s(t)$ is the steady state of the unperturbed system and $x_p(t)$ represents the waveforms of the perturbed system.

Since oscillators are periodic systems, phase shift ϕ is dependent on the time when the impulse injection is applied to the oscillator. If we sweep the impulse injection from $t = 0$ to $t = T$, we obtain a periodic waveform of phase shift $\phi(t)$, which we call the phase sensitivity waveform, and which is very important for predicting the oscillator's jitter performance. Since it is not practical to obtain the phase sensitivity waveform using impulse injection, a method for calculating it without performing the full simulation is of great value.

B. Nonlinear Oscillator Phase Macromodel

In [23], Demir *et al* put this intuition on a solid mathematical foundation. Using Floquet theory [25], [26], Demir presented the method for obtaining phase sensitivity waveforms from an oscillator's linearized periodically time varying (LPTV) systems, and formulated a nonlinear scalar differential equation to capture the oscillator's phase deviation due to perturbations.

A general oscillator under perturbation can be described by

$$\dot{x} + f(x) = b(t), \tag{10}$$

where $b(t)$ is a vector of perturbation signals applied to the free running oscillator. The corresponding LPTV system can be obtained by linearizing this oscillator about its steady state orbit:

$$\begin{aligned} \dot{w}(t) \approx & -\frac{\partial f(x)}{\partial x}|_{x_s(t)} w(t) + b(t) \\ = & A(t)w(t) + b(t), \end{aligned} \tag{11}$$

where $x_s(t)$ is the steady state orbit of the oscillator. Via Floquet decomposition of the homogeneous part of this LPTV system, a series of Floquet exponents and corresponding eigenvectors can be obtained. Since we know, from Figure 1, that phase deviation ϕ never vanishes, it should correspond to the Floquet exponent with the value of 0. [23] showed that the phase sensitivity waveform of the oscillator can be extracted from the eigenvector associated with the Floquet exponent 0, and that the phase deviation $\alpha(t)$ is governed by a simple one-dimensional nonlinear differential equation [23]

$$\dot{\alpha}(t) = V_1^T(t+\alpha(t)) \cdot b(t), \tag{12}$$

where $V_1(t)$ is the perturbation projection vector (PPV). $V_1(t)$ is a vector with the size of system size n; Each element in $V_1(t)$ represents the oscillator's phase sensitivity to the perturbation applied to the corresponding node. The PPV, or the phase sensitivity vector, has periodic waveforms that have the same frequency as that of the oscillator. Various methods [23], [27]–[29], both in the time domain and the frequency domain, have been presented for calculating the PPV from SPICE-level circuit descriptions of oscillators. In (12), the phase deviation $\alpha(t)$ has units of time. To obtain the phase deviation in radians, we need to multiply $\alpha(t)$ by the oscillator's free-running frequency ω_0.

C. Amplitude Macromodel

Once the phase deviation $\alpha(t)$ is obtained by solving (12), a macromodel for dominant amplitude components can be built as well, by linearizing the oscillator over its perturbed time-shifted orbits $x_s(t+\alpha(t))$. In [21], a method is presented to construct amplitude macromodels of oscillators. The oscillator is first linearized on $x_s(t+\alpha(t))$:

$$\begin{aligned} \dot{y}(t) &\approx -\frac{\partial f}{\partial x}|_{x_s(t+\alpha(t))} y(t) + b(t) \\ &= A(x_s(t+\alpha(t)))y(t) + b(t), \end{aligned} \tag{13}$$

where $x_s(t)$ is the oscillator's steady-state orbit, $\alpha(t)$ is the phase deviation due to perturbation $b(t)$, and $y(t)$ is a small amplitude deviation from the phase-shifted orbit, due to the perturbation $b(t)$. By introducing a new variable $\hat{t} = t + \alpha(t)$ and defining $\hat{y}(\hat{t}) = y(t)$ and $\hat{b}(\hat{t}) = b(t)$, we obtain a linear periodic time-varying (LPTV) system

$$\dot{\hat{y}}(\hat{t}) = A(x_s(\hat{t}))\hat{y}(\hat{t}) + \hat{b}(\hat{t}). \tag{14}$$

Applying Floquet decomposition, the LPTV system can be decomposed into a diagonalized LTI system with periodic input/output vectors:

$$\hat{y}(\hat{t}) = \sum_{i=1}^{n} u_i(\hat{t}) \int_0^{\hat{t}} \exp(\mu_i(\hat{t}-\tau)) v_i^T(\tau)\hat{b}(\tau)d\tau, \tag{15}$$

where μ_i are Floquet exponents, and $v_i(t)$ and $u_i(t)$ are periodic input/output vectors. By dropping the Floquet exponent corresponding to phase and other less important Floquet exponents, we obtain a reduced amplitude macromodel.

When both the phase shift $\alpha(t)$ and amplitude variations $y(t)$ are available, the oscillator's orbit under perturbation can be obtained by the equation

$$x_p(t) = x_s(t+\alpha(t)) + y(t), \tag{16}$$

where $x_s(t)$ is the steady state orbit of the oscillator, and $x_p(t)$ is the orbit of the oscillator under perturbation.

IV. Simulating Coupled Oscillators Using The Nonlinear Oscillator Macromodel

Once oscillator macromodels are obtained using the methods in Section III, the complex oscillator equations in the coupled system can be replaced with the nonlinear scalar phase equation (12), and the coupling between oscillators can be modeled as the inputs applied to (12). The resulting reduced system can be simulated using any transient simulator, with great speedups compared to the full system. Moreover, since the system is simulated in the phase domain directly, the simulation efficiency can be improved by using larger timesteps and simpler integration methods, without appreciable loss of accuracy.

A. Nonlinear Phase Equation For Coupled Systems

Since in (12) $V_1(t)$ is a vector in which each element represents the phase sensitivity of the corresponding node in the oscillator, and $b(t)$ is also a vector of size n that models the perturbation on each oscillator circuit node, our method can handle a system consisting of oscillators with different characteristics, coupled with very complex topology. For purposes of illustration of simplicity, we assume that the coupled system consists of identical oscillators, and coupling only occurs on one node with the phase sensitivity function $v(t)$ and the steady state waveform $x(t)$. This leaves the following governing equation of the coupled system:

$$\dot{\alpha}_i(t) = v(t+\alpha_i(t)) \cdot \gamma_i(t), \qquad i = 1, ..., N, \tag{17}$$

where N is the network size or number of oscillators in the coupled system, $\alpha_i(t)$ is the phase shift of oscillator i due to coupling, $v(t)$ is the phase sensitivity of the node on which coupling occurs and $\gamma_i(t)$ is the coupling function that models the coupling force applied to oscillator i. If the coupling $\gamma_i(t)$ and phase sensitivity $v(t)$ are purely sinusoidal waveforms, it is easy to show that (17) is equivalent to Kuramoto's model. However, when the coupling and the phase sensitivity functions are not purely sinusoidal, (17) is far more accurate than Kuramoto's model, since it considers all harmonics.

B. Modeling Coupling In Coupled Systems

To solve (17), we need to formulate the coupling function $\gamma_i(t)$, which models the coupling force applied to oscillator i from other oscillators in the coupled system. Here, we model three typical couplings: resistive coupling, capacitive coupling and idealized coupling, shown in Figure 2.

1) Resistively-loaded coupling: Figure 2(a) depicts a system coupled by resistors; the resistance between oscillator i and oscillator j is $R_{i,j}$ ($R_{i,j} = \infty$ if there has no coupling between oscillator i and oscillator j). Such coupling adds a load to the oscillator and this can lead to significant amplitude effects if the coupling is strong. We call this the *loading effect*. For such a system, the coupling function can be written as

$$\gamma_i(t) = \sum_{j=1}^{n} (x_j(t) - x_i(t))/R_{i,j} \tag{18}$$

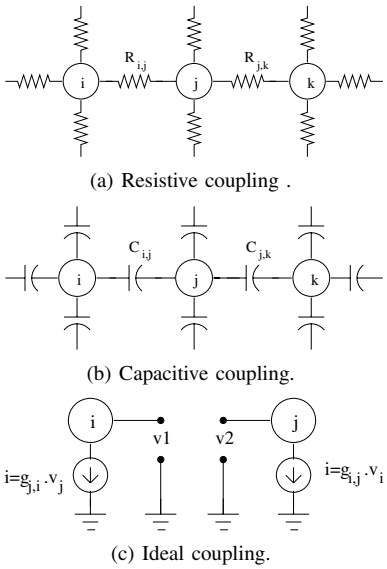

(a) Resistive coupling .

(b) Capacitive coupling.

(c) Ideal coupling.

Fig. 2. Typical coupling in coupled oscillating systems.

and models the perturbation current injected into oscillator i, where $x_j(t)$ and $x_i(t)$ are the voltage waveforms of oscillator j and oscillator i respectively. According to (16), the oscillator waveform has the form

$$x_i(t) = x(t+\alpha_i(t)) + y_i(t), \qquad i = 1,..,N, \tag{19}$$

where $x(t)$ is the oscillator's steady state waveform, $\alpha_i(t)$ is the oscillator's phase shift due to coupling, and $y_i(t)$ is the oscillator's amplitude variations due to coupling. These can be calculated using the method in [21]. In the case that the coupling is weak and the loading effect is negligible, we can ignore the amplitude variations and obtain a simpler form:

$$x_i(t) = x(t+\alpha_i(t)), \qquad i = 1,..,N. \tag{20}$$

If the coupling is not weak, the loading effect may change the free-running characteristics of the oscillator (*e.g.*, as in relaxation and ring oscillators). In such cases, Kuramoto's model cannot apply, since it assumes oscillators converge to a mean frequency that can be changed due to the loading effect.

2) Capacitively-loaded coupling: If the system is coupled by capacitors, as shown in Figure 2(b), and the capacitance between oscillator i and oscillator j is $C_{i,j}$ ($C_{i,j} = 0$ if there has no coupling between oscillator i and oscillator j), the coupling function can be written as

$$\gamma_i(t) = \sum_{j=1}^{n} C_{i,j} \cdot (\dot{x}_j(t) - \dot{x}_i(t)), \tag{21}$$

where $\dot{x}_j(t)$ and $\dot{x}_i(t)$ are derivatives of waveforms on oscillator j and oscillator i. If the oscillator waveforms have the form of (20), their derivatives can be written as

$$\dot{x}_i(t) = \dot{x}(t+\alpha_i(t)) \cdot (1+\dot{\alpha}_i(t)), \qquad i = 1,...,N. \tag{22}$$

Considering that $\dot{\alpha}(t) \ll 1$ if coupling in the system is weak, we can simplify (22) as

$$\dot{x}_i(t) = \dot{x}(t+\alpha_i(t)), \qquad i = 1,...,N \tag{23}$$

for the weak coupling case.

If the coupling is not weak, the loading effect needs to be taken into consideration, and we need to incorporate the amplitude macromodel. Furthermore, capacitive loading may change the free-running frequency of LC type oscillators, since it changes the equivalent tank capacitance. For such a system, the oscillator will not converge to a mean frequency, and Kuramoto's model fails for this case as well, since it assumes that oscillators converge to a mean frequency.

3) Idealized coupling (without loading): Figure 2(c) depicts the idealized coupling case. The coupling from oscillator j to oscillator i is modeled by coupling factor $g_{j,i}$. Such systems have no loading effect, and is thus the only case in which Kuramoto's model can apply. The coupling function can be written as

$$\gamma_i(t) = \sum_{j=1}^{n} g_{j,i} \cdot x_j(t), \qquad i = 1,...,N. \tag{24}$$

Incorporating the coupling function $\gamma(t)$ into the governing phase equation (17), we can solve the phase dynamics of complex coupled systems in this simplified form using the traditional transient integration method. Since the system size is reduced and the phase is simulated directly, we obtain speedups without appreciably sacrificing accuracy, especially in the case of large coupled systems with complex oscillator models.

V. Application to Large Oscillator Networks

In this section, we apply and evaluate our technique. We apply our method to simulate the collective behavior of different coupled oscillating systems, including nanoelectronic systems and biochemical systems. We first simulate a Brusselator system to show that our model is able to reproduce complex pattern formation processes in biochemical systems. We then apply our technique to a TPL-based CNN system to demonstrate its ability in simulating next-generation nano-scale systems. All simulations are performed using **MATLAB** on a Linux system. We construct oscillator macromodels using the method described in Section III, and simulate the behavior of different coupled systems using the method described in Section IV. Numerical results show our method is able to capture the phase and amplitude dynamics in coupled systems with good accuracy. We obtain speedups of about 3000× in our simulations.

A. Pattern formation in a Brusselator biochemical network

Patterns widely exist in many biological systems, such as animal furs and human fingerprints. The pattern formation process, which is important for the understanding of biological mechanisms in biological systems, can be modeled as a reaction-diffusion system. In such systems, chemicals interact with each other, forming patterns from an initially uniform state. The simulation of these chemical interaction systems present a challenge for direct simulation methods, as the system sizes are very large. In this section, we simulate a large Brusselator biochemical system using our macromodel-based method.

A Brusselator system is a oscillating chemical system with two chemical species,

$$\begin{aligned} \frac{\partial u}{\partial t} &= A - (B+1)u + (1+\gamma \cdot \sin(2\pi f t))u^2 v + D_u \nabla^2 u \\ \frac{\partial v}{\partial t} &= Bu - u^2 v + D_v \nabla^2 v, \end{aligned} \tag{25}$$

where u and v are two species, A and B are constant parameters corresponding to feed concentrations, $\gamma \sin(2\pi f t)$ is the external force applied to the oscillator, and D_u and D_v are the diffusion coefficients. We chose $A = 0.5$ and $B = 1.5$ in our simulations.

We simulate a network of Brusselator oscillators with size of 400×400 (about 160000 oscillators). After discretizing the diffusion between oscillators, we obtain a coupled oscillating system coupled by resistive coupling. The coupling resistance R is dependent on diffusion coefficients D_u and D_v. We show that the coupled system forms different patterns when the coupling resistance R is varied.

We first choose the coupling resistance $R = 15$, and simulate the system using our method for 150 cycles. The simulation results are shown in Figure 3, which clearly depicts the pattern formation process in this coupled oscillating system. In this figure, we use colors to represent the phase of oscillators, *i.e.*, different colors indicate oscillators with different phases. At the beginning ($t = 0$), all oscillators are given a random phase: hence we cannot see any pattern. After 5 oscillating cycles ($t = 5T$), the collective synchronization phenomenon is clearly seen: oscillators synchronize their phase with the phase of their neighbors. As a result, we can see many color spots in the figure. After 20 oscillating cycles, some small target patterns appear, and a spiral wave pattern forms on the right side of the figure. From $t = 40T$ onwards, we can see those patterns grow, and merge together. Finally, after 150 cycles, we obtain a complex figure which combines both target pattern and spiral pattern. This pattern is very close to the experimental measurements reported in [8], [11].

Now we investigate the patterns of this biological system under different coupling strength, and plot the patterns in Figure 4. In the

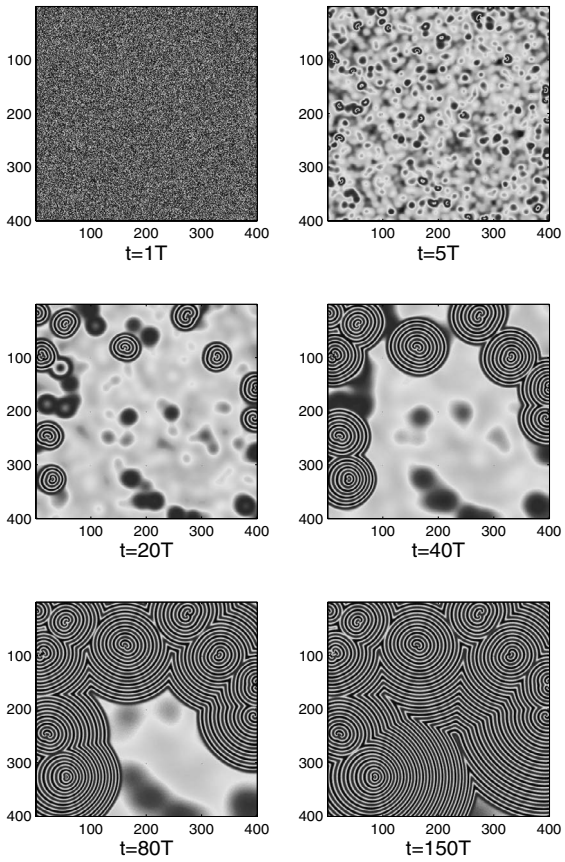

Fig. 3. Pattern formation in an unforced biochemical system.

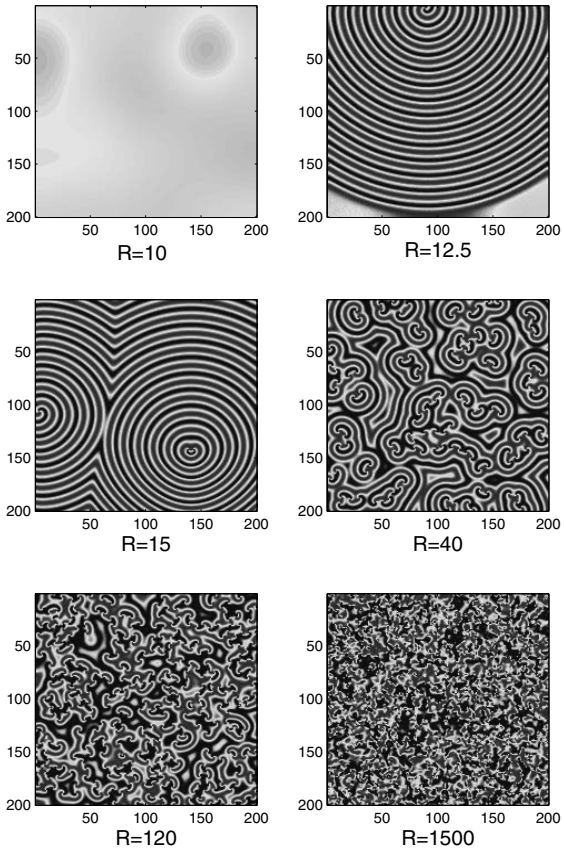

Fig. 4. Biological patterns under different coupling strength.

first figure, coupling is strong ($R = 10$), all oscillators lock to same phase, so we cannot see any pattern. In the second figure, we increase the coupling resistance to $R = 12.5$, a spiral wave pattern forms. We keep increasing the coupling resistance and obtain different kinds of patterns, as shown in Figure 4.

Such pattern formation processes are of great importance in biochemical systems, suggesting new insights in the understanding of biological processes. Our macromodel based technique offers a feasible approach for simulating the pattern formation in large biochemical systems. We obtain about $3000\times$ speedup in this simulation. If the system size is larger and oscillator model is more complex, speedups can be greater.

B. Nanoelectronic System – Tunneling Phase Logic Based Cellular Nonlinear Network

Figure 5 depicts a basic tunneling phase logic unit and its oscillating waveform. A basic TPL unit consists of an ultra-small SET junction with capacitance C_j, a DC bias V_{DC} and a pump voltage V_p. The SET junction has the property that when its voltage increases to a threshold V_T, single-electron tunneling occurs and the capacitor C_j is discharged. With the DC bias V_{DC} providing a bias current, the SET junction behaves as shown in Figure 5(b). The AC pump provides a sinusoidal voltage with amplitude V_p, which runs two times faster than the SET frequency. Therefore, if the SET is super-harmonically locked by the pump voltage, it has two steady states, with the phase difference π. If the phase of the SET oscillator is set to represent the logical values 0 and 1, we can realize logic in phase, instead of voltage as in traditional CMOS circuits.

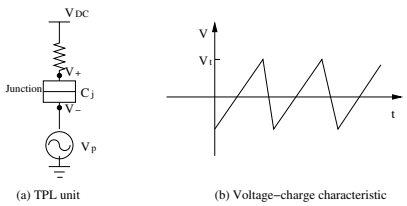

Fig. 5. TPL unit and its voltage-charge characteristic.

We first use the nonlinear phase macromodel to verify bistability in the TPL. We simulate multiple TPL units with random initial phases, using the nonlinear phase equation (12). If the TPL has a bistable nature, the final phase of those TPL units will converge to two phases with the interval of π. We plot the simulation results in Figure 6. Four TPL units have different phases at $t = 0$. After about 20 cycles, the phases of TPL unit 1 and unit 4 converge to about $\frac{3\pi}{2}$; and the phases of TPL unit 2 and unit 3 converge to about $\frac{\pi}{2}$. Hence, our simulations verify that the TPL does indeed feature bistability.

In [3], a TPL based CNN implementation is proposed. Here, we use our macromodel based technique to simulate the TPL-CNN system. We adopt the near-neighbor coupling topology described in [3], and define the nonlinear output of the TPL unit as

$$f_{i,j}(\phi_{i,j}) = \begin{cases} 1, & \pi < \phi_{i,j} < 2\pi \\ -1, & 0 < \phi_{i,j} < \pi, \end{cases} \tag{26}$$

where $f_{i,j}$ is the output of the TPL cell on row i and column j, and

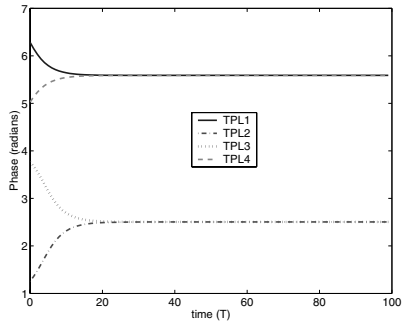

Fig. 6. The bistability of the TPL.

$\phi_{i,j}$ is the cell's phase.

A major potential application of CNNs is in image processing [30]. Here we present an example to show the image processing ability of TPL-CNNs: we use a TPL-CNN to detect an image edge. The original images are shown in Figure 7(a) and Figure 7(b). We transfer these images into two-color mode and apply them as inputs to the CNN network. In Figure 7(c) and Figure 7(d), we can see tunneling occurs and the inputs are replicated at the outputs of the CNN after 4 oscillating cycles. At $t = 8T$, the edges of the images are detected, as shown in Figure 7(e) and Figure 7(f).

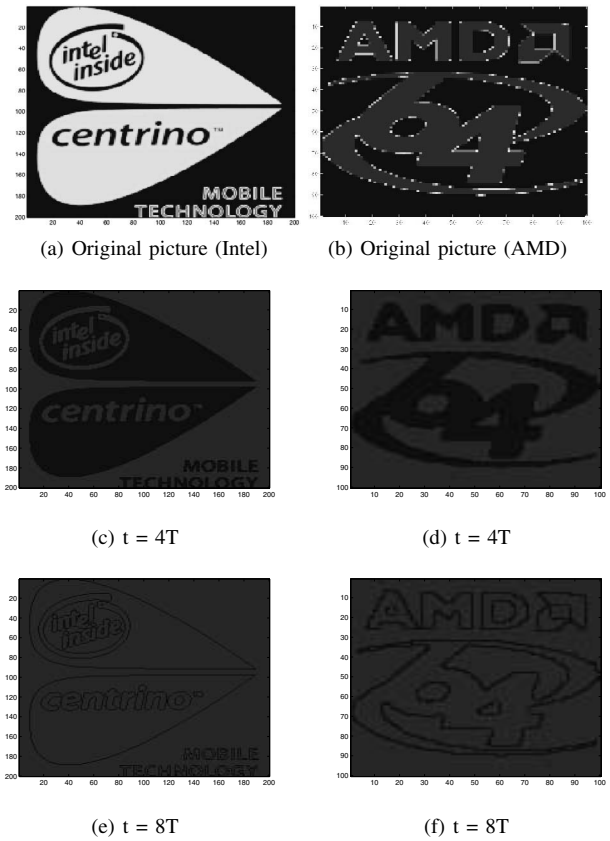

(a) Original picture (Intel) (b) Original picture (AMD)

(c) t = 4T (d) t = 4T

(e) t = 8T (f) t = 8T

Fig. 7. Image edge detection performed by a TPL-CNN.

VI. Conclusion

We extend a nonlinear oscillator macromodelling technique, usually applied to the prediction of phase noise in electrical systems, to nano- and biochemical-systems, and demonstrate its ability in solving some difficult problems in these areas. Experimental results show that our technique is able to predict the behavior of very large-scale coupled oscillating systems, with great speedups while preserving the simulation accuracy. Our future work includes investigating large-scale oscillating systems under external forces.

References

[1] T. Ohshima and R. A. Kiehl. Operation of bistable phase-locked single-electron tunneling logic elements. J. Appl. Phys., April 1996.

[2] R. A. Kiehl and T. Ohshima. Bistable locking of single-electron tunneling elements for digital circuitry. Appl. Phys. Lett., 67(17):2494–2496, Oct 1995.

[3] Tao Yang, R. A. Kiehl, and L. O. Chua. Tunneling phase logic cellular nonlinear networks. International Journal of Bifurcation and chaos, 11:2895–2911, 2001.

[4] L. O. Chua and L. Yang. Cellular neural networks: Theory. IEEE Trans. Circuit and Systems, pages 1257–1272, 1988.

[5] L. O. Chua and L. Yang. Cellular neural networks: Applications. IEEE Trans. Circuit and Systems, pages 1273–1290, 1988.

[6] A. J. Koch and H. Meinhardt. Biological pattern formation: from basic mechanisms to complex structures. Rev. Mod. Phys., 66:1481–1507, OCT 1994.

[7] D. A. Kessler and H. Levine. Pattern formation in dictyostelium via the dynamics of cooperative biological entities. Phys. Rev. E, 48:4801–4804, Dec 1993.

[8] P. K. Maini, K. J. Paintera, and H. N. P. Chaub. Spatial pattern formation in chemical and biological systems. J. Chem. Soc., Faraday T rans., pages 3601–3610, 1997.

[9] A. M. Turing. Philos. T rans. R. Soc. London, 1952.

[10] I. Prigogine and R. Lefever. J. Chem. Phys., 48:1695, 1968.

[11] A. L. Lin, A. Hagberg, A. Ardelea, M. Bertram, H. L. Swinney, and E. Meron. Four-phase patterns in forced oscillator systems. Physical Review E, 62:3790–3798, 2000.

[12] A. L. Lin, M. Bertram, K. Martinez, and H. L. Swinney. Resonant phase patterns in a reaction-diffusion system. Physical Review Letters, 84:4240–4243, May 2000.

[13] R.L. Schiek and E.M. May. Examining tissue differentiation stability through large scale, multi-cellular pathway modeling. In Nanotech 2005, May 2005.

[14] Tim Poston. Catastrophe Theory And Its Applications. Dover Publications, 1997.

[15] L. Nagel. SPICE2: A Computer Program to Simulate Semiconductor Circuits. Electron. Res. Lab., Univ. Calif., Berkeley, 1975.

[16] N. Wiener. Nonlinear Problems in Random Theory. MIT press, Cambridge, MA, 1958.

[17] N. Wiener. Cybernetics. MIT press, Cambridge, MA, 1961.

[18] A. T. Winfreei. Biological rhythms and the behavior of populations of coupled oscillators. J. Theor. Biol., 1967.

[19] Y. Kuramoto. Chemical Oscillations, Waves, and turbulence. Springer, Berlin, 1984.

[20] Y. Kuramoto and I. Nishikawa. Cooperative Dynamics in Complex Physical systems. Springer, Berlin, 1989.

[21] X. Lai and J. Roychowdhury. Automated oscillator macromodelling techniques for capturing amplitude variations and injection locking. In IEEE/ACM International Conference on Computer Aided Design, November 2004.

[22] Tosiya Taniuti and Nobuo Yajima. Perturbation method for a nonlinear wave modulation. Journal of Mathematical Physics, 10:1369–1372, Aug 1969.

[23] A. Demir, A. Mehrotra, and J. Roychowdhury. Phase noise in oscillators: a unifying theory and numerical methods for characterization. IEEE Trans. on Circuits and Systems-I:Fundamental Theory and Applications, 47(5):655–674, May 2000.

[24] X. Lai and J. Roychowdhury. Capturing Oscillator Injection Locking via Nonlinear Phase-Domain Macromodels. IEEE Trans. Microwave Theory Tech., 52(9):2251–2261, September 2004.

[25] R. Grimshaw. Nonlinear Ordinary Differential Equations. Blackwell Scientific, New York, 1990.

[26] M. Farkas. Periodic Motions. Springer-Verlag, New York, 1994.

[27] A. Demir. Phase noise in oscillators: Daes and colored noise sources. In IEEE/ACM International Conference on Computer-Aided Design, November 1998.

[28] A. Demir, D. Long, and J. Roychowdhury. Computing phase noise eigenfunctions directly from steady-state jacobian matrices. In IEEE/ACM International Conference on Computer Aided Design, pages 283–288, November 2000.

[29] A. Demir and J. Roychowdhury. A reliable and efficient procedure for oscillator ppv computation, with phase noise macromodelling applications. IEEE Trans. on Computer-Aided Design of Integrated Circuits and Systems, 22(2):188–197, February 2003.

[30] T. Roska and J. Vandewalle. Cellular Neural Networks. Wiley, New York, 1993.